Energy-Corrected Finite Element Methods for Scalar Elliptic Problems

Thomas Horger, Markus Huber, Ulrich Rüde, Christian Waluga, and Barbara Wohlmuth

Abstract In this work, we consider the finite element solution of several scalar elliptic problems with singularities in two dimensions. We outline recent theoretical developments in energy corrected approaches and demonstrate numerically that by local and easy to implement modifications of the discrete operators, optimal convergence orders in weighted Sobolev norms can be recovered.

1 Introduction

We consider boundary value problems in an open and bounded domain $\Omega \subset \mathbb{R}^2$, involving the second order linear elliptic operator

$$L := -\mathrm{div}(K\nabla u),$$

where $0 < K_0 \leq K \in L^\infty(\Omega)$ is a known coefficient, e.g., a diffusivity or the permeability of a porous medium. If not mentioned otherwise, we will set $K = 1$ for simplicity. However, we will also consider the case of a heterogeneous coefficient having jumps. It is known that numerical methods applied to such problems often suffer from suboptimal convergence due to singularities in the solution which dictate the regularity. In this paper, we consider modified finite element methods that allow to deal with singular solution components in an efficient and effective way.

T. Horger • C. Waluga (✉) • B. Wohlmuth
Institute for Numerical Mathematics, Technische Universität München, Boltzmannstraße 3, 85748 Garching b. München, Germany
e-mail: horger@ma.tum.de; waluga@ma.tum.de;wohlmuth@ma.tum.de

M. Huber • U. Rüde
Universität Erlangen-Nürnberg, Lehrstuhl für Informatik 10, Cauerstraße 11, 91058 Erlangen, Germany
e-mail: markus.huber@fau.de; ulrich.ruede@fau.de

A. Abdulle et al. (eds.), *Numerical Mathematics and Advanced Applications - ENUMATH 2013*, Lecture Notes in Computational Science and Engineering 103, DOI 10.1007/978-3-319-10705-9_2

As a first example for such singularities, we consider the case of a non-convex Lipschitz domain Ω having a re-entrant corner with interior angle $\pi < \theta < 2\pi$. In general, the solution to the problem

$$Lu = f \quad \text{in } \Omega, \qquad u = 0 \quad \text{on } \partial\Omega \tag{1}$$

will then be composed of smooth components as well as singular components of type $s_k = r^{k\pi/\theta} \sin(k\pi/\theta\phi)$, $k \in \mathbb{N}$, where ϕ denotes the angle in polar coordinates, and r stands for the distance to the re-entrant corner of Ω. This can be observed even when the data are smooth [18,23,27]. While the convergence order in the H^1-norm is the same as the order of the best approximation, this does not hold for the L^2-norm, where a gap of $1 - \pi/\theta$ can be observed due to the non-smoothness of the singular component $s_1 \notin H^\alpha(\Omega)$, $\alpha \geq 1 + \pi/\theta$. This effect is commonly referred to as *pollution* [9, 10, 32]. A similar, but even worse situation occurs in interface problems, see, e.g., [21, 22], when the interfaces between subdomains $\Omega_i \subset \Omega$ with different coefficient K intersect in one point. Here we typically see singular components of type r^ϵ, $0 < \epsilon \ll 1$.

In the literature, many different approaches have been proposed to deal with singular solution components, such as graded meshes [2], the enrichment of the finite element space with singular functions [6, 9, 13, 14, 16, 26, 32], or first order system least squares approaches, which add discrete versions of the singular basis functions to standard finite element spaces in a least-squares framework [7, 8, 11, 17, 24].

Most of the aforementioned approaches have in common the aim to improve the finite element approximation nearby the singularity. However, in some applications, the quantity of interest can be computed by excluding or relaxing the influence of the neighborhood of the singularities, e.g., stress intensity factors, eigenvalues or the flux at some given interface not including the singular points. Here, an accurate representation of the solution is not required near the singularity. This motivates the use of energy correction schemes that do not enrich the finite element spaces [20,30, 31, 33]. The basic idea was originally introduced in the context of finite difference methods in [31, 33] and applied to finite elements in [29]. It was then analyzed in [20] for more general meshes, and it was proved that a careful modification of the energy in the original method can drastically improve the convergence. In the following, we briefly sketch the main ideas.

2 Re-entrant Corners

We consider a weak form of the boundary value problem (1). The corresponding bilinear form is given by $a(v, w) := \int_\Omega \nabla v \cdot \nabla w \, \mathrm{d}x$, $v, w \in H^1(\Omega)$. To define the energy correction, we introduce $a_{i,h}(v, w) := \int_{\omega_{i,h}} \nabla v \cdot \nabla w \, \mathrm{d}x$, where $\omega_{i,h}$ denotes the union of the ith layer of elements in $\mathcal{T}_h$ around the re-entrant corner x_c, i.e.,

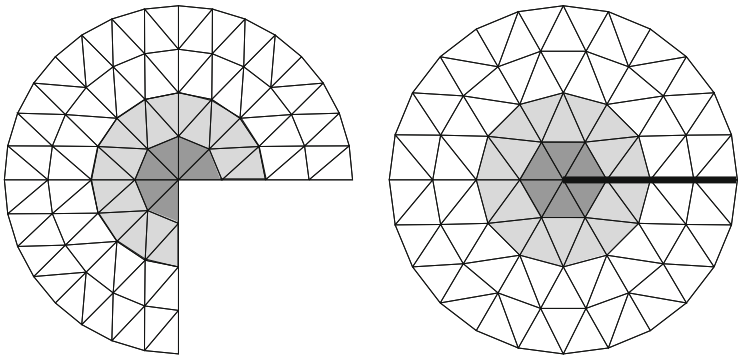

Fig. 1 *left*: Triangulation of the circular L-shape domain with $\theta = \frac{3\pi}{2}$; *right*: circular slit domain with $\theta = 2\pi$. The elements marked in *dark gray* belong to $\omega_{1,h}$ and the elements in *light gray* are in $\omega_{2,h}$

$\omega_{1,h} := \bigcup_{T\in\mathcal{T}_h, x_c\in\partial T} \overline{T}$ and $\omega_{i,h} := \bigcup_{T\in\mathcal{T}_h, \partial T\cap\overline{\omega}_{i-1,h}\neq\emptyset} \overline{T}$ for $i > 1$; cf. Fig. 1 for some illustration. Here $\mathcal{T}_h$ stands for a family of quasi-uniform simplicial meshes with mesh-size h. For given $\gamma \in \mathbb{R}^n$, $n \in \mathbb{N}$ fixed, we then define the bilinear form

$$a_{ec}(v, w) := a(v, w) - \sum\nolimits_{i=1}^{n} \gamma_i \, a_{i,h}(v, w). \tag{2}$$

The energy-corrected finite element form of (1) then reads: Find $u_h(\gamma) \in V_h^p$ s.t.

$$a_{ec}(u_h(\gamma), v) = (f, v), \quad v \in V_h^p, \tag{3}$$

where $(\cdot,\cdot)$ denotes the standard L^2-scalar product, and $V_h^p \subset H_0^1(\Omega)$ is the conforming piecewise polynomial finite element space of degree $p > 0$ associated with $\mathcal{T}_h$. For $\gamma = 0$ the standard finite element solution is recovered. As we will see in Sect. 3, our approach is not restricted to Dirichlet boundary conditions but also applies for Neumann boundary conditions. Note that the Laplace operator can be used to model a membrane, i.e., the effect of the modification with the parameters γ can be regarded as a softening ($\gamma_i \in (0, 1)$) or stiffening ($\gamma_i < 0$) of the material in the vicinity of the re-entrant corner.

The modification (2) does not change the structure of the stiffness matrix. Hence, it is cheap and easy to implement into existing codes, provided that γ_i and $\omega_{i,h}$ are known. Theoretical results for linear finite elements [20] require that we apply the correction in a union of elements $\omega_h \subset B_{k_0 h}$, where $B_{k_0 h}$ is a ball with radius $k_0 h$ and k_0 sufficiently large, with center at the re-entrant corner. Numerical results show that fixing $n = 1$ and setting $\omega_h = \omega_{i,h}$ is sufficient for the case $p = 1$, see also [30]. Our choice of $\omega_{i,h}$ is motivated by this observation indicating that for one parameter $\gamma \in [0, 1)$, it is sufficient to impose the correction only in those elements directly attached to the singularity.

We emphasize that, different from other techniques, the number of nodes affected by the correction will not depend on h as long as n does not depend on h. For simplicity, we assume that the layers $\omega_{i,h}$ are mirror-symmetric with respect to the singular point if $\theta \geq \frac{3}{2}\pi$. Otherwise, we would possibly have to consider more correction parameters, since then some terms in the analysis will not cancel by symmetry arguments.

2.1 A Nested Newton Algorithm

Let us first consider the case of linear finite elements and set $n = 1$: Assuming that the union of elements defined by $\omega_{1,h}$ is large enough, the quality of $u_h(\gamma) \in V_h^1$ is only determined by the choice of γ. In [20] it has been shown that for each $h > 0$ a proper subinterval of $[0, 1)$ exists such that no pollution occurs, and second order convergence in a suitably-weighted Sobolev norm can be recovered. The length of the subinterval tends to zero as the mesh-size does. Thus asymptotically exactly one correction parameter exists such that optimality can be observed. Here, we define the correction parameter as the unique root of the non-linear scalar-valued *energy defect function*

$$g_h(\gamma) := a(s_1, s_1) - a_{ec}(s_{1,h}(\gamma), s_{1,h}(\gamma)), \qquad \text{for } \gamma \in \mathbb{R}. \tag{4}$$

where we recall that s_1 denotes the first singular function and $s_{1,h}(\gamma)$ its modified finite element approximation. In [30] we developed and analyzed Newton algorithms for the calculation of an accurate enough correction parameter γ in a multi-level context. Such methods will be used frequently in the numerical results in this article to determine suitable correction parameters.

Next, we consider the extension to quadratic finite elements (or, analogously, linear elements on non-symmetric meshes) and $n = 2$. It turns out that a good choice of $\gamma \in \mathbb{R}^2$ is the root of the vector-valued energy defect function

$$g_h(\gamma) := \begin{pmatrix} a(s_1, s_1) - a_{ec}(s_{1,h}(\gamma), s_{1,h}(\gamma)) \\ a(s_2, s_2) - a_{ec}(s_{2,h}(\gamma), s_{2,h}(\gamma)) \end{pmatrix}, \qquad \text{for } \gamma \in \mathbb{R}^2. \tag{5}$$

By similar considerations as in the case of one parameter, we can derive a nested one-step Newton algorithm on a family of uniformly refined meshes $\mathcal{T}_l$. The mesh $\mathcal{T}_{l+1}$ is obtained by decomposing each element of $\mathcal{T}_l$ into four sub-elements. Given the initial guess $\gamma_0 = (0, 0) \in (-1, 1)^2$ on the coarse mesh $\mathcal{T}_0$, we set for $l = 0, 1, \ldots$

$$\gamma_{l+1} = [\nabla g_h(\gamma_l)]^{-1} \begin{pmatrix} a(s_{1,h}(\gamma_l), s_{1,h}(\gamma_l)) - a(s_1, s_1) \\ a(s_{2,h}(\gamma_l), s_{2,h}(\gamma_l)) - a(s_2, s_2) \end{pmatrix}, \tag{6}$$

with

$$\nabla g_h(\gamma) = \begin{pmatrix} a_{1,h}(s_{1,h}(\gamma), s_{1,h}(\gamma)) & a_{2,h}(s_{1,h}(\gamma), s_{1,h}(\gamma)) \\ a_{1,h}(s_{2,h}(\gamma), s_{2,h}(\gamma)) & a_{2,h}(s_{2,h}(\gamma), s_{2,h}(\gamma)) \end{pmatrix}. \tag{7}$$

Note that the index l denotes the refinement level, and on each level typically only one Newton step is carried out. The start value for the Newton on level $l+1$ is the value computed on level l. For the nested one-step Newton method we see that

$$[g_h]_i = \mathscr{O}\left(h^{\frac{2i\pi}{\omega}}\right) \qquad \text{and} \qquad [\nabla g_h]_{ij}^{-1} = \mathscr{O}\left(h^{\frac{-2j\pi}{\omega}}\right),$$

hence $\gamma_{l+1} \in \mathscr{O}(1)$, i.e., the values of γ stay bounded independent of the mesh-level. However, a detailed analysis of this algorithm is beyond the scope of this paper.

In the following section, we demonstrate the efficiency of the nested Newton method in numerical experiments.

2.2 Numerical Examples with Second Order Elements

In the following examples, we consider the Poisson problem in a circular domain with re-entrant corners of angle $\theta = \frac{3}{2}\pi$ and $\theta = 2\pi$ and assume that $\omega_{1,h}$ is mirror-symmetric on the coarsest mesh. We set a homogeneous right hand side and Dirichlet boundary conditions are chosen such that the exact solution is given by $u = s_1 + s_2 + s_3$. Note that the third singular component does not reduce the convergence rates of the uncorrected approach due to sufficient regularity. We conduct our numerical experiments on a series of uniformly refined meshes (cf. Fig. 1 for the initial triangulations and correction domains) and compare the errors of corrected vs. uncorrected finite elements in weighted L^2 norms

$$\|u - u_h\|_{0,\alpha} := \|r^\alpha (u - u_h)\|_{L^2(\Omega)}, \tag{8}$$

where $r = |x - x_c|$ denotes the distance to the re-entrant corner x_c, and α is the weighting parameter. Note that for $\alpha = 0$ we recover the standard L^2 norm. In each case, the roots of the energy correction function (5) are determined by the nested Newton-method discussed above where the initial guess on level 0 is always set to zero. The contour lines of the energy correction function for the initial meshes are plotted in Fig. 2. The bullet in the pictures denotes the unique root of the energy correction function.

The correction parameters for the L-shape and slit domain are listed in Table 1. As it can be seen easily both parameters converge with respect to the level and for both domains $\gamma_{1,opt}$ is positive while $\gamma_{2,opt}$ is negative.

In our convergence study, we consider $p = 2$ and different choices of the correction parameter for illustration, namely, the energy correction with the level-

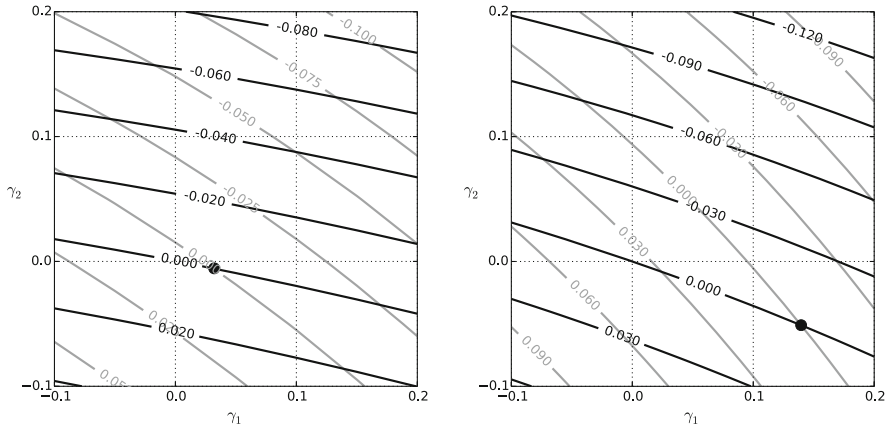

Fig. 2 Contour lines and root (*bullet*) of the energy functional (5) in the L-shape (*left*) and slit domain (*right*); *gray lines* are associated with the first and *black* ones with the second component of the energy functional

Table 1 Approximate roots of $g_h(\gamma)$ obtained by a nested Newton method applied to subsequent refinements of the respective initial meshes of Fig. 1

Level	$\gamma_{1,opt}$	$\gamma_{2,opt}$
1	0.0320706	−0.0055412
2	0.0315346	−0.0055392
3	0.0315229	−0.0055351
4	0.0315208	−0.0055342
L-shape		

Level	$\gamma_{1,opt}$	$\gamma_{2,opt}$
1	0.1493019	−0.0497673
2	0.1395878	−0.0510151
3	0.1395358	−0.0510148
4	0.1395348	−0.0510143
Slit		

dependent parameters of Table 1, and the choice $(\gamma_1, 0.0)$ with γ_1 determined by the one-step Newton method of [30]. Moreover, we compare the standard quadratic finite element method resulting from the choice $(\gamma_1, \gamma_2) = (0.0, 0.0)$ as well as two manually chosen values, where one is closer to the actual optimal parameter than the other. The latter experiments are given to demonstrate that the energy correction can yield solutions of much better quality by manual fine-tuning of parameters, even when the actual asymptotically correct values are unknown.

In Tables 2 and 3, we list the results of our convergence study for the L-shape and slit domains, respectively. The errors are measured in the weighted L^2 norm with weighting $\alpha \approx 1.38$ for the L-shape and $\alpha \approx 1.55$ for the slit.

In both cases, we observe that the asymptotically optimal convergence order of $\mathcal{O}(h^3)$ is only recovered for the correction approach with both parameters chosen according to the root of the energy defect function. Restricting the correction to only one parameter, however, still improves the rate to $\mathcal{O}(h^2)$, since the effects of the stronger singularity s_1 can still be compensated by this simpler correction. From the results for the manually tuned parameters it can be concluded that our approach can significantly improve the quality of the solution, even when the exact parameters are

Table 2 L-shape: Errors $10^4 \times \|u - u_h(\gamma_1, \gamma_2)\|_{0,\alpha \approx 1.38}$ for different parameters

(γ_1, γ_2)	$(\gamma_{1,opt}, \gamma_{2,opt})$		$(\gamma_2, 0)$		$(0, 0)$		$(0.031, -0.005)$		$(0.02, -0.006)$	
Level	Error	Rate	Error	Rate	Error	Rate	Error	Rate	Error	Rate
1	1.8697	–	1.9402	–	4.9912	–	1.7893	–	2.8886	–
2	0.2031	3.20	0.2843	2.77	1.9475	1.36	0.2017	3.10	1.0433	1.47
3	0.0240	3.08	0.0425	2.74	0.7716	1.34	0.0257	2.94	0.4100	1.35
4	0.0030	3.00	0.0064	2.72	0.3061	1.33	0.0047	2.46	0.1625	1.34

Table 3 Slit domain: Errors $10^3 \times \|u - u_h(\gamma_1, \gamma_2)\|_{0,\alpha \approx 1.55}$ for different parameters

(γ_1, γ_2)	$(\gamma_{1,opt}, \gamma_{2,opt})$		$(\gamma_2, 0)$		$(0, 0)$		$(0.139, -0.051)$		$(0.15, -0.06)$	
Level	Error	Rate	Error	Rate	Error	Rate	Error	Rate	Error	Rate
1	1.1790	–	1.3055	–	2.4165	–	1.0874	–	1.2833	–
2	0.1372	3.10	0.2994	2.12	1.1968	1.01	0.1372	2.99	0.1749	2.88
3	0.0168	3.03	0.0738	2.02	0.5966	1.00	0.1720	3.00	0.0312	2.49
4	0.0021	3.02	0.0184	2.01	0.2978	1.00	0.0275	2.65	0.0112	1.48

unknown. However, to observe optimal asymptotic convergence rates, we require a high accuracy of the parameter on the finer meshes. Let us remark here that for multiple re-entrant corners, the correction parameters can be determined by solving local problems for each corner in a preprocessing step. The optimal correction parameters depends on the interior angle, as already seen from the numerical results, but also on $\omega_{1,h}$. More precisely, the number and the local shape of elements in $\omega_{1,h}$ influence the optimal correction parameters.

3 Eigenvalue Problems

Next, we consider the eigenvalue problem with homogeneous Neumann boundary conditions

$$Lu_m = \lambda_m u_m \qquad \text{in } \Omega.$$

As before, we choose an L-shaped domain $\Omega := (-1, 1)^2 \backslash ([0, 1] \times [-1, 0])$ and a slit-domain $\Omega := (-1, 1)^2 \backslash ([0, 1] \times \{0\})$ for our numerical results. For comparison with reference values given in the literature [12, 19], we use different meshes in this example. Moreover, we also present results for a domain with multiple re-entrant corners, in which case we compute a reference solution on a finer mesh. The meshes are always constructed such that we obtain perfectly symmetric isosceles triangles around the singular points; cf. Fig. 3.

It is well-known from the literature [3–5, 12, 25], that the above mentioned pollution effect can be observe, but that it occurs only for all eigenfunctions and eigenvalues, for which a non-smooth singular component is present. For sufficiently

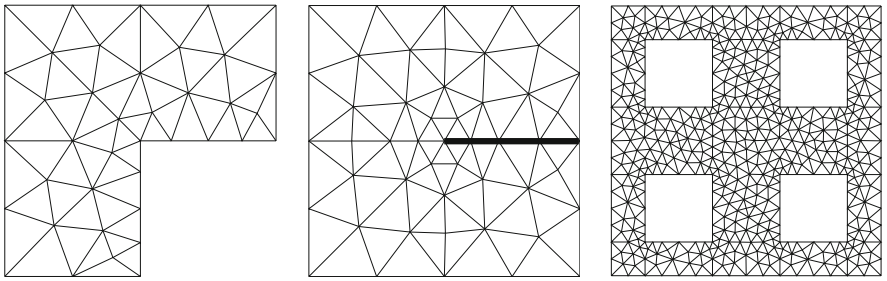

Fig. 3 L-shape, slit, and domain with multiple re-entrant corners

smooth eigenfunctions, a quadratic convergence rate for the eigenvalues can be observed in case of linear finite elements, i.e., $p = 1$.

Our modified finite element formulation reads: find the discrete eigenvalues $\lambda_{m,h} \in \mathbb{R}$ and the eigenfunctions $u_{h,m}(\gamma) \in V_h^1$ such that

$$a_{ec}(u_{h,m}(\gamma), v) = \lambda_{h,m}(u_{h,m}(\gamma), v), \quad v \in V_h^1, \tag{9}$$

where $0 \leq \lambda_{h,1} \leq \lambda_{h,2} \leq \ldots$. For simplicity of notation, we use the same symbol as before for the finite element space although no homogeneous boundary conditions are imposed on the space. Let us next briefly outline the convergence analysis for this modified scheme.

3.1 Convergence Analysis

In this subsection, we focus on the convergence analysis of the discrete eigenvalues $\lambda_{h,m}$ and follow the lines of [28] in the conforming setting. To do so, we introduce the eigenvalue problem: find $\lambda \in \mathbb{R}$ and $w \in H^1(\Omega)$ such that $a(w, z) = \lambda(w, z)$ for all $z \in H^1(\Omega)$. The non-negative eigenvalues are ordered such that $0 \leq \lambda_1 \leq \lambda_2 \leq \ldots$, and the associated eigenfunctions are denoted by w_i with the normalization $(w_i, w_j) = \delta_{i,j}$. Now define the m-dimensional space V_m by $V_m := \text{span}\{w_i, i \leq m\}$. Further for each $v \in V_m$ let the modified Galerkin projection R_h onto V_h^1 be defined by $a_{ec}(R_h v, v_h) = a(v, v_h)$ for all $v_h \in V_h^1$. We recall that R_h depends on the specific choice of γ. In terms of R_h, we define $E_{m,h} := R_h V_m$ and note that $\dim E_{m,h} = m$ for $h \leq h_0$ small enough.

For the sake of presentation, let us first state the main result and subsequently develop the ingredients needed for its proof.

Theorem 1 *Let* $1 - \frac{\pi}{\omega} < \alpha < 1$. *If the above mentioned modification is used with* $n = 1$ *and* γ_{opt}, *the following upper and lower bound for* $\lambda_{h,m}$ *hold,*

$$\lambda_m(1 - Ch^2\lambda_m^{1+\alpha}) \leq \lambda_{h,m} \leq \lambda_m(1 + Ch^2\lambda_m^{\alpha+1}).$$

Our proof is based on the following two technical results which are provided without a detailed proof.

Lemma 1 *Let* $1 - \frac{\pi}{\omega} < \tilde{\alpha} < \alpha < 1$ *then it holds*

$$\|r^{-\tilde{\alpha}} v\|_0 \leq C \|v\|_0^{1-\alpha} \|v\|_1^{\alpha}, \quad v \in H^1(\Omega).$$

The upper bound in Lemma 1 can be obtained by using the Hölder inequality in combination with interpolation arguments and standard Sobolev embedding results. Combining Lemma 1 with [28, Lemma 6.4-2], [20, Theorem 2.4] and some straightforward computations yield the following bounds.

Lemma 2 *Let* $v \in V_m$ *with* $(v, v) = 1$. *Then* $v = \sum_{i=1}^m \beta_i w_i$ *with* $\sum_{i=1}^m \beta_i^2 = 1$, *and it satisfies* $a(v, z) = (f_v, z)$ *for all* $z \in H^1(\Omega)$ *with* $f_v := \sum_{i=1}^m \beta_i \lambda_i w_i$. *Moreover, we have* $r^{-\alpha} f_v \in L^2(\Omega)$ *for* $1 - \frac{\pi}{\omega} < \alpha < 1$, *and the following bounds hold with constants independent of the mesh-size*

$$|a(v, v) - a_{ec}(R_h v, R_h v)| \leq C h^2 \lambda_m^{2+\alpha},$$
$$(R_h v, R_h v) \geq 1 - C h^2 \lambda_m^{\alpha+1}.$$

Now we are prepared to provide the proof of the main result.

Proof (Theorem 1) The proof is based on the characterization of the eigenvalues by the Rayleigh quotient. We start with the upper bound. Using $E_{h,m}$ as defined above together with Lemma 2, we get the following upper bound:

$$\begin{aligned}
\lambda_{h,m} &\leq \max_{v \in E_{m,h}} \frac{a_{ec}(v, v)}{(v, v)} = \max_{v \in V_m} \frac{a_{ec}(R_h v, R_h v)}{(R_h v, R_h v)} \\
&= \max_{v \in V_m} \frac{a(v, v) + a_{ec}(R_h v, R_h v) - a(v, v)}{(R_h v, R_h v)} \\
&= \max_{v \in V_m} \frac{a(v, v)}{(v, v)} \max_{v \in V_m} \frac{(v, v)}{(R_h v, R_h v)} + \max_{v \in V_m} \frac{a_{ec}(R_h v, R_h v) - a(v, v)}{(R_h v, R_h v)} \\
&\leq \lambda_m \frac{1 + C h^2 \lambda_m^{2+\alpha}}{1 - C h^2 \lambda_m^{\alpha+1}} \lesssim \lambda_m (1 + C h^2 \lambda_m^{\alpha+1}) + C h^2 \lambda_m^{2+\alpha} (1 + C h^2 \lambda_m^{\alpha+1}).
\end{aligned}$$

As next step it remains to show the lower bound. In contrast to the uncorrected scheme, we do not have the trivial bound $\lambda_m \leq \lambda_{m,h}$. The proof of the lower bound follows basically the lines of the upper bound but requires the use of a different m-dimensional space. Firstly we define a new space given by $E_m := \operatorname{span}\{\widetilde{w}_i, i \leq m\}$ where $\tilde{w}_i \in H^1(\Omega)$ is defined by $a(\tilde{w}_i, z) = (w_{i,h}, z)$ for all $z \in H^1(\Omega)$. Secondly, we note that $R_h E_m = E_{m,h}$ and thus for h small enough we have $\dim E_m = m$.

Now, similar arguments as before yields

$$\begin{aligned}\lambda_m &\leq \max_{v\in E_m} \frac{a(v,v)}{(v,v)} = \max_{v\in E_m} \frac{a_{ec}(R_h v, R_h v) + a(v,v) - a_{ec}(R_h v, R_h v)}{(v,v)} \\ &= \max_{v\in E_m} \frac{a_{ec}(R_h v, R_h v)}{(R_h v, R_h v)} \max_{v\in E_m} \frac{(R_h v, R_h v)}{(v,v)} + \max_{v\in E_m} \frac{a(v,v) - a_{ec}(R_h v, R_h v)}{(v,v)} \\ &\leq \lambda_{h,m}(1 + Ch^2 \lambda_{h,m}^{1+\alpha}).\end{aligned}$$

Combining the upper bounds for λ_m and $\lambda_{h,m}$ yields the lower bound for $\lambda_{h,m}$. □

The steps outlined in this section show the flexibility and potential of the ideas of [20, 30] to eigenvalue problems. A more detailed analysis provides also optimal bounds for the eigenfunction convergence. Let us next support our theoretical ideas by numerical results.

3.2 Numerical Computation of Eigenvalues

We conduct convergence studies for the eigenvalue problem defined on the geometries depicted in Fig. 3. We first compare the numerical results obtained without correction to those obtained with a suitable modification parameter.

In this example, we make use of the Neumann fit tabulated in [30, Table 5.3], which provides a simple heuristic approach to determine modification parameters in case of meshes consisting of isosceles triangles around the singularity. This purely geometric assumption is satisfied for our meshes by construction (see Fig. 3).

The correction parameter γ for the L-shape ($\theta = \frac{3}{2}\pi$) and the multiple re-entrant corners domain is given by $\gamma \approx 0.1478$. We note that in each case four isosceles triangles are attached to the singularity, and thus the correction parameter is the same for all re-entrant corners. For the slit domain ($\theta = 2\pi$), we count six adjacent elements at the singular vertex, and hence we determine our correction parameter to $\gamma \approx 0.2716$ (more precise values are given in the respective tables).

In Tables 4–6 we list the results for our convergence study for the L-shape, the slit domain and the domain with multiple re-entrant corners, respectively. Without correction, we observe suboptimal rates for some eigenvalues in each of the three cases. However, using the modified method, the asymptotically optimal convergence of $\mathcal{O}(h^2)$ for all given eigenvalues is obtained in the three cases. Note that we excluded the results for some eigenvalues for the slit domain in Table 5. This is because the corresponding eigenfunctions do not include singular components strong enough to affect the optimal rate for linear elements. Hence, for these eigenvalues, a convergence rate of $\mathcal{O}(h^2)$ can be reached already by using the non-corrected method.

Table 4 Convergence rates for eigenvalues in the L-shaped domain with and without energy correction

No correction $\gamma = 0$:										
	1.EV		2.EV		3.EV		4.EV		5.EV	
	Exact: 1.47562		Exact: 3.53403		Exact: 9.86960		Exact: 9.86960		Exact: 11.38948	
Level	Value	Rate	Value	Rate	Value	Rate	Value	Rate	Value	Rate
1	1.55008	–	3.63939	–	10.79641	–	10.90447	–	12.67323	–
2	1.50014	**1.60**	3.56116	1.96	10.10623	1.97	10.12814	2.00	11.71975	1.96
3	1.48402	**1.55**	3.54091	1.98	9.92994	1.97	9.93496	1.98	11.47442	1.96
4	1.47861	**1.49**	3.53576	1.99	9.88483	1.99	9.88604	1.99	11.41101	1.98
5	1.47672	**1.44**	3.53447	2.00	9.87342	2.00	9.87372	2.00	11.39489	1.99
Correction $\gamma = 0.147850426060652$:										
	1.EV		2.EV		3.EV		4.EV		5.EV	
	Exact: 1.47562		Exact: 3.53403		Exact: 9.86960		Exact: 9.86960		Exact: 11.38948	
Level	Value	Rate	Value	Rate	Value	Rate	Value	Rate	Value	Rate
1	1.51075	–	3.62603	–	10.78432	–	10.89390	–	12.64990	–
2	1.48457	**1.97**	3.55913	1.87	10.10560	1.95	10.12758	1.99	11.71674	1.95
3	1.47785	**2.00**	3.54060	1.93	9.92990	1.97	9.93493	1.98	11.47396	1.95
4	1.47617	**2.03**	3.53571	1.96	9.88482	1.99	9.88604	1.99	11.41094	1.98
5	1.47575	**2.06**	3.53446	1.98	9.87342	2.00	9.87372	2.00	11.39488	1.99

Table 5 Convergence rates for eigenvalues in the slit domain with and without energy correction

No correction $\gamma = 0$:										
	1.EV		2.EV		5.EV		7.EV		8.EV	
	Exact: 1.03407		Exact: 2.46740		Exact: 9.86960		Exact: 12.26490		Exact: 12.33701	
Level	Value	Rate	Value	Rate	Value	Rate	Value	Rate	Value	Rate
1	1.14032	–	2.52918	–	10.78301	–	13.97705	–	14.17015	–
2	1.07951	**1.23**	2.48307	1.98	10.10730	1.94	12.75729	**1.80**	12.81216	1.95
3	1.05478	**1.13**	2.47135	1.99	9.93045	1.97	12.43849	**1.50**	12.44434	2.15
4	1.04392	**1.07**	2.46839	2.00	9.88497	1.99	12.32633	**1.50**	12.36411	1.99
5	1.03887	**1.04**	2.46765	2.00	9.87346	1.99	12.28924	**1.34**	12.34381	1.99
Correction $\gamma = 0.271607294328175$:										
	1.EV		2.EV		5.EV		7.EV		8.EV	
	Exact: 1.03407		Exact: 2.46740		Exact: 9.86960		Exact: 12.26490		Exact: 12.33701	
Level	Value	Rate	Value	Rate	Value	Rate	Value	Rate	Value	Rate
1	1.06167	–	2.49235	–	10.76626	–	13.85168	–	13.88581	–
2	1.04116	**1.96**	2.47377	1.97	10.10651	1.92	12.66340	**1.99**	12.73749	1.95
3	1.03583	**2.01**	2.46902	1.97	9.93041	1.96	12.36581	**1.98**	12.43961	1.96
4	1.03449	**2.06**	2.46781	1.99	9.88497	1.98	12.29021	**1.99**	12.36294	1.98
5	1.03417	**2.14**	2.46750	1.99	9.87346	1.99	12.27120	**2.01**	12.34352	1.99

Table 6 Convergence rates for eigenvalues in the domain with multiple re-entrant corners with and without correction

No correction $\gamma = 0$:										
	1.EV		2.EV		3.EV		4.EV		5.EV	
	Exact: 0.11422		Exact: 0.11422		Exact: 0.23460		Exact: 0.31626		Exact: 0.31626	
Level	Value	Rate	Value	Rate	Value	Rate	Value	Rate	Value	Rate
1	0.11609	–	0.11609	–	0.23841	–	0.32303	–	0.32323	–
2	0.11489	1.48	0.11489	1.48	0.23595	1.51	0.31861	1.53	0.31867	1.53
3	0.11446	1.46	0.11446	1.46	0.23509	1.47	0.31709	1.49	0.31711	1.50
4	0.11431	1.42	0.11431	1.42	0.23478	1.44	0.31656	1.45	0.31657	1.45
5	0.11425	1.39	0.11425	1.39	0.23467	1.40	0.31637	1.41	0.31637	1.42
Correction $\gamma = 0.147850426060652$:										
	1.EV		2.EV		3.EV		4.EV		5.EV	
	Exact: 0.11422		Exact: 0.11422		Exact: 0.23460		Exact: 0.31626		Exact: 0.31626	
Level	Value	Rate	Value	Rate	Value	Rate	Value	Rate	Value	Rate
1	0.11472	–	0.11473	–	0.23574	–	0.31869	–	0.31887	–
2	0.11435	1.85	0.11436	1.85	0.23492	1.85	0.31690	1.92	0.31695	1.92
3	0.11425	1.97	0.11425	1.96	0.23469	1.96	0.31642	1.99	0.31643	1.99
4	0.11422	2.04	0.11422	2.03	0.23462	2.02	0.31630	2.04	0.31630	2.03
5	0.11422	2.11	0.11422	2.10	0.23461	2.09	0.31627	2.09	0.31627	2.08

4 Jumping Coefficients

Next, let us study the influence of heterogeneous coefficients with jumps. We consider again the scalar elliptic problem (1) but in contrast to the previous sections, we now assume that K is piecewise constant on disjoint subsets $\Omega_i \subset \Omega := (-1,1)^2$, i.e., we define $\Omega_1 := (0,1)^2$, $\Omega_2 := (-1,0) \times (0,1)$, $\Omega_3 := (-1,0)^2$ and $\Omega_4 := (0,1) \times (-1,0)$, and set $K = 1$ in Ω_2, Ω_4 and $K = a$ in Ω_1, Ω_3 for finite $a > 0$. Whenever $a \neq 1$ one obtains a discontinuity at the origin, which causes solutions in $H^{1+\epsilon}(\Omega)$ for $0 < \epsilon < 1$ and possibly $\epsilon \ll 1$; cf. [15, 21]. As before, this severely limited regularity bound results in poor L^2-accuracy of the uncorrected discrete solutions. The solution of (1) again admits a singular function representation, with singular components of the form

$$s_k(r,\phi) = r^{\lambda_k}\theta_k(\phi), \quad \lambda_k \leq \lambda_{k+1}, k \in \mathbb{N}. \tag{10}$$

Here the exponent λ_k can be determined with help of an auxiliary Sturm–Liouville eigenvalue problem [15]. We note that (r,ϕ) are the polar coordinates with respect to the origin $(0,0)$. Typically, the exponent λ_1 is very small, i.e., $\lambda_1 \ll 1$, which renders s_1 as the dominating singular component in the problem. Since by [21, Lemma 3.3] there holds $\lambda_1 + \lambda_2 = 2$ for the case outlined above, the energy

correction with only one correction parameter per singular vertex is feasible. Hence, we introduce a modification of the weak form at the singularity by

$$a_{ec}(v, w) := \int_{\Omega} K\nabla v \cdot \nabla w \, \mathrm{d}x - \gamma \int_{\omega_h} K\nabla v \cdot \nabla w \, \mathrm{d}x. \tag{11}$$

where $\gamma \in [0, 1)$, and ω_h is a union of elements in $\mathscr{T}_h$. As before, we choose ω_h as the union of those elements adjacent to the vertex at which the singularity is located. The modified finite element method for (1) is then again given in the form of (3), and the corrections are again determined as the root of the energy functional (4). We remark that a similar correction has been proposed to recover optimal multigrid convergence rates for elliptic problems with intersecting interfaces in [1].

4.1 Numerical Results

As a first benchmark, we consider non-homogeneous Dirichlet boundary conditions such the exact solution is given by $u = s_1$. We conduct a convergence study on a series of uniformly refined meshes and, as before, we compare the energy corrected approach to the standard finite element method. The first two mesh levels and correction domains are depicted in Fig. 4 for illustration.

We consider two values of a, i.e., $a = 10$ and $a = 1{,}000$, and in a preprocessing step we solve the Sturm–Liouville problem to obtain the first eigenvalue as $\lambda_1 \approx 0.38996$ and $\lambda_1 \approx 0.04025$, respectively. The other singular components are of higher regularity (i.e., $s_i \in H^2(\Omega), i > 1$) and are therefore not considered in the following. For both cases we then approximate the roots of the energy defect function (4) by a classical Newton method until the relative error between two consecutive iterates is at most $1.48 \cdot 10^{-8}$. The results are listed in Fig. 5 alongside with nonlinear fits against the function $\gamma_\infty + ch^{2(1-\lambda_1)}$. For $a = 1{,}000$, we observe

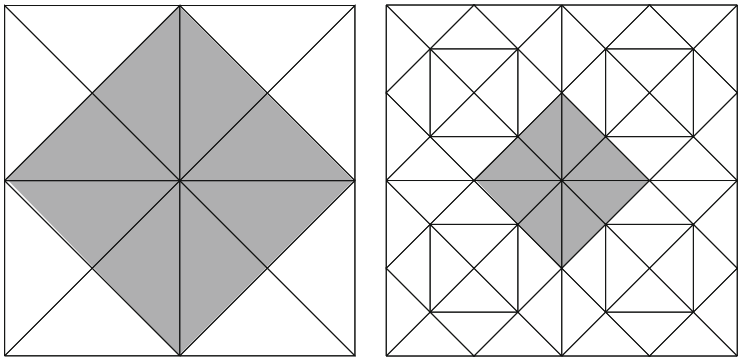

Fig. 4 Mesh levels 1 and 2 of the unit square with correction domains ω_h in *gray*

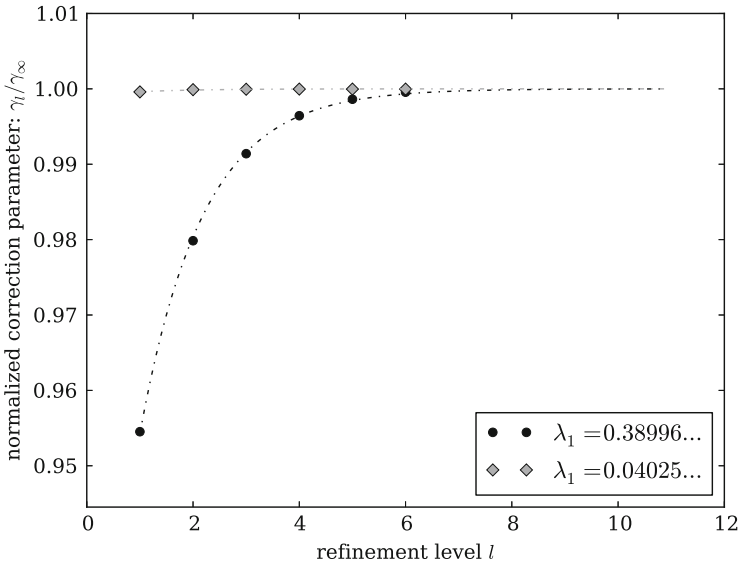

	level	1	2	3	4	5	6
$a = 10$	γ_{opt}	0.38848	0.39879	0.40349	0.40554	0.40643	0.40681
$a = 1000$	γ_{opt}	0.93576	0.93604	0.93609	0.93611	0.93611	0.93611

Fig. 5 Approximate roots of the energy defect function (4) obtained on subsequent refinements of the initial meshes of Fig. 4 for jumping material coefficients. *Dashed lines* indicate the nonlinear fits against the function $\gamma_\infty + ch^{2(1-\lambda_1)}$

Table 7 Errors $10^2 \times \|u - u_h(\gamma)\|_{0,\alpha \approx 0.66004}$ for jumping coefficients with $a = 10$

γ	γ_{opt}		0		0.406		0.3		0.5	
Level	Error	Rate	Error	Rate	Error	Rate	Error	Rate	Error	Rate
1	2.72860	–	3.06090	–	2.71390	–	2.80460	–	2.63900	–
2	0.71951	1.92	1.38890	1.14	0.71293	1.93	0.84889	1.72	0.68297	1.95
3	0.18359	1.97	0.69770	0.99	0.18253	1.97	0.29198	1.54	0.23705	1.53
4	0.04636	1.99	0.37922	0.88	0.04627	1.98	0.13016	1.17	0.11776	1.01
5	0.01170	1.99	0.21420	0.82	0.01175	1.98	0.06939	0.91	0.06718	0.81
6	0.00295	1.99	0.12297	0.80	0.00301	1.96	0.03938	0.82	0.03924	0.78

that the convergence of γ_{opt} with respect to the refinement level is much faster than for $a = 10$. This is in accordance with the theoretical results for re-entrant corners of [30], which state that the convergence is faster in case of stronger singularities (Table 7).

Again, for both cases, we conduct a convergence study in which we compare the modified and standard finite element solutions, as well as three heuristic choices. For $a = 10$, we measure the error in the weighted L^2-norm with $\alpha \approx 0.66004$. For the modified approach with correction parameters as listed in Fig. 5, an optimal

convergence rate of $\mathcal{O}(h^2)$ is obtained, while the convergence of the standard finite element method is clearly limited due to the singular components. For the manually tuned choices we again observe that the solution quality is much better than without correction. Although on coarse meshes nearly optimal rates can only be seen for the choice $\gamma = 0.406$, which is close enough to the optimal values of Fig. 5, asymptotically the convergence rate will deteriorate. This effect can be seen more dominantly for the choices $\gamma = 0.3$ and $\gamma = 0.5$. A not optimal choice of γ will yield asymptotically the same poor convergence rate as the uncorrected method has.

For comparison, we list the results for the case $a = 1{,}000$ in Table 8, where the error is measured in the weighted L^2-norm with $\alpha \approx 0.96475$. Also here we see that using the previously determined parameters an optimal asymptotic convergence rate is recovered despite the strongly singular component.

Finally, let us consider a more complex numerical example in $\Omega = [-2, 2] \times [-2, 2]$. We define $i = \lfloor x \rfloor$ and $j = \lfloor y \rfloor$, and set

$$K = \begin{cases} 1{,}000 & \text{if } (-1)^{i+j} > 0, \\ 1 & \text{if } (-1)^{i+j} < 0, \end{cases}$$

thus, we identify 9 singularities which are corrected as depicted in Fig. 6. The boundary conditions are chosen as $u = 1$ on the bottom boundary, $u = 0$ on the top and $\nabla u \cdot \mathbf{n} = 0$ elsewhere.

Table 8 Errors $10^2 \times \|u - u_h(\gamma)\|_{0,\alpha \approx 0.96475}$ for jumping coefficients with $a = 1{,}000$

γ	γ_{opt}		0		0.936		0.9		0.95	
Level	Error	Rate	Error	Rate	Error	Rate	Error	Rate	Error	Rate
1	0.41774	–	0.51892	–	0.43095	–	0.43531	–	0.42932	–
2	0.11332	1.88	0.32494	0.68	0.11944	1.85	0.12422	1.81	0.11825	1.86
3	0.02917	1.96	0.24001	0.44	0.03142	1.93	0.03725	1.74	0.03178	1.90
4	0.00738	1.98	0.19177	0.32	0.00813	1.95	0.01876	0.99	0.01073	1.57
5	0.00186	1.99	0.15902	0.27	0.00209	1.96	0.01587	0.24	0.00704	0.61
6	0.00047	1.99	0.13485	0.24	0.00054	1.96	0.01475	0.11	0.00637	0.14

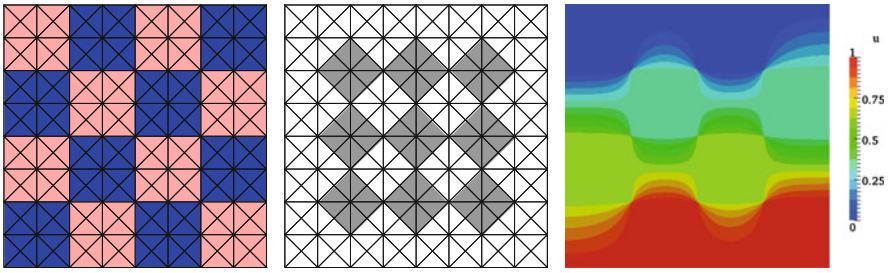

Fig. 6 *Left*: coefficient $K = 1$ (*dark*), $K = 1{,}000$ (*light*); *center*: correction on level 1 in *light gray*; *right*: reference solution (with energy correction on level 8)

Table 9 Errors $10 \times \|u - u_h(\gamma)\|_{0,\alpha \approx 0.96475}$; Convergence analysis of the energy correction method and standard finite element method for the example with 9 singularities

γ	γ_{opt}		0	
Level	Error	Rate	Error	Rate
1	0.50254	–	1.15720	–
2	0.09690	2.07	0.92582	0.32
3	0.02472	1.97	0.77083	0.26
4	0.00636	1.96	0.65581	0.23

Due to the construction of the jumping coefficient K each of the 9 singularities has the same first eigenvalue $\lambda_1 = 0.04025$, thus, also the correction parameter in the neighborhood of each singularity has the same value, namely, $\gamma \approx 0.93611$. Since we have no exact solution at hand for this example, we compute a reference solution with the energy corrected method on a high resolution mesh for comparison. In Table 9, we study the convergence to the reference solution, starting with the mesh of Fig. 6. The error is measure in a weighted L^2 norm with a weight of $\alpha \approx 0.96475$ around each singularity. Again, we observe optimal convergence rates for the energy corrected method. Hence, the correction parameters for each singularity arising in a practical application can be determined independently in a preprocessing step.

Conclusion

In this work, we discussed the extension of energy corrected finite element methods from the special case of linear finite elements on domains with re-entrant corners to second order finite elements, eigenvalue problems, and singularities resulting from jumping material parameters in two space dimensions. We demonstrated that given the correction parameters, the modified methods can dramatically improve the numerical solutions in presence of strong singular solution component. Quasi-optimal convergence rates are recovered. Hence, they provide an appealing alternative to graded or adaptive meshes and function space enrichment for applications in which a high accuracy in vicinity of the singular regions is not required.

Acknowledgements Financial support by the "Deutsche Forschungsgemeinschaft" through grant WO-671/13-1 is gratefully acknowledged.

References

1. R.E. Alcouffe, A. Brandt, J.E. Dendy Jr., J.W. Painter, The multi-grid method for the diffusion equation with strongly discontinuous coefficients. SIAM J. Sci. Stat. Comput. **2**(4), 430–454 (1981)
2. T. Apel, A. Sändig, J. Whiteman, Graded mesh refinement and error estimates for finite element solutions of elliptic boundary value problems in non-smooth domains. Math. Methods Appl. Sci. **19**, 63–85 (1996)
3. I. Babuška, B. Guo, J. Osborn, Regularity and numerical solution of eigenvalue problems with piecewise analytic data. SIAM J. Numer. Anal. **26**(6), 1534–1560 (1989)
4. I. Babuška, J. Osborn, Finite element-Galerkin approximation of the eigenvalues and eigenvectors of selfadjoint problems. Math. Comput. **52**(186), 275–297 (1989)
5. ———, Eigenvalue problems, in *Handbook of Numerical Analysis*, vol. 2 (North Holland, Amsterdam, 1991), pp. 643–787
6. I. Babuška, M. Rosenzweig, A finite element scheme for domains with corners. Numer. Math. **20**, 1–21 (1972)
7. M. Berndt, T. Manteuffel, S. McCormick, Analysis of first-order system least-squares (FOSLS) for elliptic problems with discontinuous coefficients: part II. SIAM J. Numer. Anal. **42**, 409–436 (2005)
8. M. Berndt, T. Manteuffel, S. McCormick, G. Starke, Analysis of first-order system least-squares (FOSLS) for elliptic problems with discontinuous coefficients: part I. SIAM J. Numer. Anal. **42**, 386–408 (2005)
9. H. Blum, M. Dobrowolski, On finite element methods for elliptic equations on domains with corners. Computing **28**, 53–63 (1982)
10. H. Blum, R. Rannacher, Extrapolation techniques for reducing the pollution effect of reentrant corners in the finite element method. Numer. Math. **52**, 539–564 (1988)
11. P. Bochev, M. Gunzburger, Finite element methods of least-squares type. SIAM Rev. **40**(4), 789–837 (1998)
12. D. Boffi, Finite element approximation of eigenvalue problems. Acta Numer. **19**(01), 1–120 (2010)
13. M. Bourlard, M. Dauge, M.-S. Lubuma, S. Nicaise, Coefficients of the singularities for elliptic boundary value problems on domains with conical points iii. Finite element methods on polygonal domains. SIAM J. Numer. Anal. **29**, 136–155 (1992)
14. S. Brenner, Multigrid methods for the computation of singular solutions and stress intensity factors. I: corner singularities. Math. Comput. **68**(226), 559–583 (1999)
15. S. Brenner, L. Sung, Multigrid methods for the computation of singular solutions and stress intensity factors. III: interface singularities. Comput. Methods Appl. Mech. Eng. **192**, 4687–4702 (2003)
16. Z. Cai, S. Kim, A finite element method using singular functions for the Poisson equation: corner singularities. SIAM J. Numer. Anal. **39**, 286–299 (2001)
17. C. Cox, G. Fix, On the accuracy of least squares methods in the presence of corner singularities. Comput. Math. Appl. **10**, 463–475 (1984)
18. M. Dauge, *Elliptic Boundary Value Problems on Corner Domains: Smoothness and Asymptotics of Solutions* (Springer, Berlin, 1988)
19. ———, Benchmark computations for Maxwell equations (2003). http://perso.univ-rennes1.fr/monique.dauge/benchmax.html
20. H. Egger, U. Rüde, B. Wohlmuth, Energy-corrected finite element methods for corner singularities. SIAM J. Numer. Anal. **52**(1), 171–193 (2014)
21. R.B. Kellogg, On the Poisson equation with intersecting interfaces. Appl. Anal. **4**(2), 101–129 (1974)
22. R. Kellogg, Singularities in interface problems, in *Numerical Solution of Partial Differential Equations, II (SYNSPADE 1970): Proceedings of the Symposium*, University of Maryland, College Park, 1970 (1971), pp. 351–400

23. V. Kondratiev, Boundary value problems for elliptic equations in domains with conical or angular points. Trans. Mosc. Math. Soc. **16**, 227–313 (1967)
24. E. Lee, T. Manteuffel, C. Westphal, Weighted norm first-order system least-squares (FOSLS) for problems with corner singularities. SIAM J. Numer. Anal. **44**, 1974–1996 (2006)
25. X. Liu, S. Oishi, Verified eigenvalue evaluation for the Laplacian over polygonal domains of arbitrary shape. SIAM J. Numer. Anal. **51**, 1634–1654 (2013)
26. J.M.-S. Lubuma, K.C. Patidar, Towards the implementation of the singular function method for singular perturbation problems. Appl. Math. Comput. **209**, 68–74 (2009)
27. V.G. Maz´ja, B.A. Plamenevskii, The coefficients in the asymptotic expansion of the solutions of elliptic boundary value problems to near conical points. Dokl. Akad. Nauk SSSR **219**, 286–289 (1974)
28. P. Raviart, J. Thomas, *Introduction à l'analyse numérique des équations aux dérivées partielles* (Masson, Paris, 1983)
29. U. Rüde, Local corrections for eliminating the pollution effect of reentrant corners. Technical report TUM-INFO-02-89-I01, Institut für Informatik, Technische Universtät München, 1989
30. U. Rüde, C. Waluga, B. Wohlmuth, Nested Newton strategies for energy-corrected finite element methods. SIAM J. Sci. Comput. **36**(4), A1359–A1383 (2014). doi: 10.1137/130935392
31. U. Rüde, C. Zenger, On the treatment of singularities in the multigrid method, in *Multigrid Methods II*, ed. by W. Hackbusch, U. Trottenberg. Lecture Notes in Mathematics, vol. 1228 (Springer, Berlin/Heidelberg, 1986), pp. 261–271. 10.1007/BFb0072651
32. G. Strang, G. Fix, *An Analysis of the Finite Element Method*, 2nd edn. (Wellesley-Cambridge Press, Wellesley, 2008)
33. C. Zenger, H. Gietl, Improved difference schemes for the Dirichlet problem of Poisson's equation in the neighbourhood of corners. Numer. Math. **30**, 315–332 (1978)